Organic & Biomolecular Chemistry

Cite this: *Org. Biomol. Chem.*, 2011, **9**, 6163

www.rsc.org/obc

PAPER

Mechanism of intramolecular catalysis in the hydrolysis of alkyl monoesters of 1,8-naphthalic acid†

Bruno S. Souza, Santiago F. Yunes, Marcelo F. Lima, José C. Gesser, Marcus M. Sá, Haidi D. Fiedler and Faruk Nome*

Received 11th April 2011, Accepted 3rd June 2011
DOI: 10.1039/c1ob05574g

Hydrolysis of alkyl 1,8-naphthalic acid monoesters **1a–d** is subject to highly efficient intramolecular nucleophilic catalysis by the neighboring COOH group. The reactivity for the COOH reaction depends on the leaving group pK_a, with values of β_{LG} of –0.50, consistent with a mechanism involving rate determining breakdown of tetrahedral addition intermediates. The release of the steric strain of the *peri*-substitiuents in the highly reactive alkyl 1,8-naphthalic acid monoesters is fundamental to understand the observed special reactivity in this intramolecular reaction. DFT calculations show how the proton transfers involved in the cleavage of the neutral ester can be catalyzed by solvent water, thus facilitating the departure of poor alkoxide leaving groups.

1. Introduction

Attempts to understand enzyme catalysis at the molecular level have led chemists to study systems involving medium effects and intramolecular catalysis in ester and amide hydrolysis, as simple models for the corresponding enzyme reactions.[1] Intramolecular "models" and enzyme reactions both involve reactions between groups brought together in a single molecule or complex.[2] The early observation of essential carboxyl groups in the catalytic centers of aspartic acid-based enzymes generated continuing interest in the possible roles of these groups in catalyzing hydrolysis reactions.[3]

As previously discussed, general acid–base catalysis is highly efficient in enzyme active sites, but in only a handful of model systems. A particularly efficient intramolecular model system is the phosphate transfer from the 8-dimethylammonium-naphthyl-1-phosphate monoanion **8DMNP**$^-$ to water and to a range of nucleophiles, which shows general acid catalysis by the neighboring NH$^+$ group, with a strong intramolecular hydrogen bond in the transition state (Scheme 1).[4] The substantial acceleration (of the order of 10^6-fold at 39 °C) is achieved by the concerted action of an internal general acid and an external nucleophile, in a reaction with low sensitivity to the incoming nucleophile.

In an attempt to detect catalysis by the carboxyl group in the hydrolysis of unactivated esters rather than *p*-nitrophenyl phosphate esters, we used the naphthalene ring as a template to build an efficient intramolecular reaction site. Relative accelerations (EMs), obtained by comparisons of second and first order rate constants, can be as large as 10^{11} in model systems based upon naphthalic acid derivatives.[5] The spontaneous hydrolysis of the 2′,2′,2′-trifluoroethyl monoester of 1,8-naphthalic acid **1a** has been shown to involve the monoanion **1a**$^-$ reacting *via* a tetrahedral intermediate **2a**$^-$ to form naphthalic anhydride (**NA**). **NA** is in slow equilibrium with naphthalic acid (**3**) in water, but the rate constant for its formation at pH 5 is *ca.* 2500 times faster than that for its hydrolysis (Scheme 2).[5b]

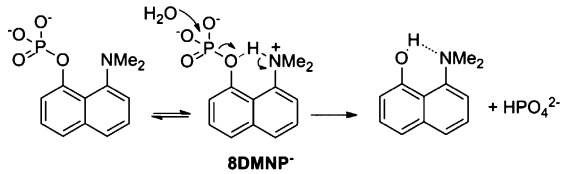

Scheme 1 Dissociative mechanism for the hydrolysis of the monoester **8DMNP**$^-$.

The remarkably high rate of reaction of the monoester monoanion **1a**$^-$ derives from the special configuration of the substrate, in which group proximity restricts solvation, and there is important relief of torsional (eclipsing) strain on formation of the fused tricyclic system.[5b] In this work we examine the remarkably rapid hydrolysis of a series of simple alkyl monoesters of 1,8-naphthalic acid **1a–d** (Scheme 2), where participation of a neighboring COOH group is fundamental and the results contribute to our understanding of reactivity in biological systems.

2. Results and discussion

Rates of decomposition of 1,8-naphthalic monoalkyl esters **1a–d** were followed by monitoring UV-vis spectral changes in the

Departamento de Química, Universidade Federal de Santa Catarina, Florianópolis-SC, Brazil. E-mail: faruk@qmc.ufsc.br; Fax: +55-48 3721-6850; Tel: +55-48 3721-6849

† Electronic supplementary information (ESI) available: Spectra for acid hydrolysis, Eyring plot for hydrolysis of the alkyl esters, UV-vis titration of the methyl ester and Cartesian coordinates of the B3LYP optimized structures together with relevant calculated information. HPLC analyses of the kinetic samples. See DOI: 10.1039/c1ob05574g

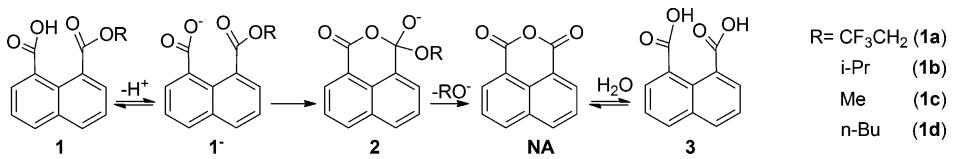

Scheme 2 Decomposition of alkyl monoesters (**1**) of 1,8-naphthalic acid (**3**).

range of 280 to 380 nm. An example of the similar changes observed in the UV spectra during the hydrolysis of all four monoalkylesters **1a–d** is given in Fig. S1 in the Supporting Information.†The absorption maxima at 298 and 340 nm have been attributed to the monoalkyl esters of naphthalic acid and to 1,8-naphthalic anhydride 3, respectively.[5] UV spectral changes show that the reaction proceeds with formation of 1,8-naphthalic anhydride (**NA**), which subsequently equilibrates with naphthalic acid following previously described pH-dependent decomposition kinetics. Nevertheless, rate constants for the intramolecular transacylation can be obtained without interference from the anhydride hydrolysis reaction.[5]

Building on our experience in reaction mechanism studies using MS techniques,[6] we applied ESI-MS to monitor the course of the hydrolysis of some of the slower reactions in aqueous solution and Fig. 1 shows the results obtained with the monoalkylester **1c**. In the ESI-MS process used here, solvated ions are "fished" directly from solution and transferred to the gas phase. The data provide snapshots of the ions present in the reaction solution, which have been shown in numerous cases to reflect accurately the actual ionic composition.[6a] At pH 5.8 and 50 °C, samples of reaction solution, containing all reagents, intermediates, and products, were transferred directly to the gas phase and characterized by ESI(±)-MS/MS. Initially, ESI-MS-(/MS) hydrolysis of **1c** showed the deprotonated form of the reactant **1c** of *m/z* 229 which reacts forming neutral 1,8-naphthalic anhydride (NA) and the monoanion of naphthalic acid of *m/z* 215. Fig. 1B, shows the decrease in concentration of **1c** as a function of time calculated from the ESI(−)-MS experiments and the results yield rate constants basically identical to those obtained by UV-vis spectroscopy (Fig. 2).

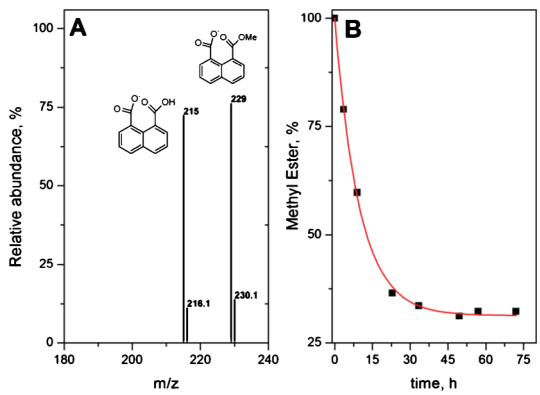

Fig. 1 (A) Typical mass spectrum for the hydrolysis of the methyl ester **1c** after 7 h of reaction. (B) Decomposition of **1c** at pH 5.80, 50 °C followed by ESI-MS.

The pH-rate profiles for these reactions (Fig. 2) exhibit two distinct regions, below and above pH 1, and the contribution of

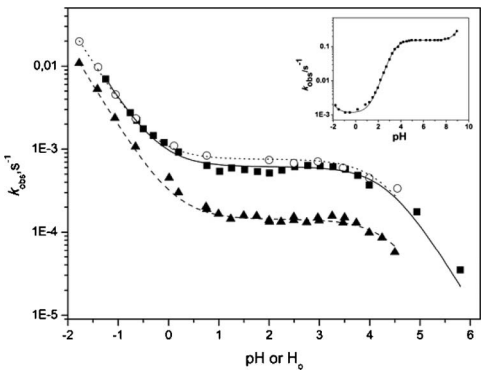

Fig. 2 First order rate constants *vs.* pH for the hydrolysis of the isopropyl (**1b**, ▲), methyl (**1c**, ■) and *n*-butyl (**1d**, ○) monoesters of 1,8-naphthalic acid, at 50.0 °C (values below zero on the pH axis correspond to the H_0 function). Curves are calculated according to eqn (1), using the rate constants given in Table 1. The insert shows the pH rate profile for the hydrolysis of the trifluoroethyl ester **1a** at 20 °C.

hydroxide ion catalysis is not significant in the pH-range (<6) under study.[5] Between $H_0 = -2$ and pH 1 the reaction shows behavior typical for specific acid catalysis; while between pH 1 and 6 the first-order rate constants show a plateau between pH 1 and 3 and for higher pH values the rate constants decrease for compounds **1b**, **1c** and **1d**. This is not normal behavior for alkyl esters, and is *prima facie* evidence for neighboring group participation. Rate constants for the intramolecular reaction of the monoalkyl esters **1a–d** as a function of pH (Fig. 2) show that the participation of the COOH group is more efficient for the more basic leaving groups, while the carboxylate anion is the most reactive species in the reaction of the 2′,2′,2′-trifluoroethyl monoester of 1,8-naphthalic acid **1a** (Scheme 3).[5b] The decrease in reactivity of the alkyl monoesters **1b–d** at higher pH is certainly related to the ionization of the carboxylic acid moiety, which is a less effective catalyst than the protonated form and the more basic leaving groups seem to be cleaved more efficiently *via* general acid catalysis. This issue will be discussed later in the text.

The series of reactions shown in Scheme 3 account satisfactorily for the kinetic observations shown in Fig. 2 and allow the derivation of eqn (1), which describes the pH dependence of the experimental first order rate constant.

$$k_{obs} = \frac{(k_{COOH} + k_H[H^+])}{(1 + K_{a2}/[H^+])} + \frac{k_{COO^-}}{(1 + [H^+]/K_{a2})} \quad (1)$$

In eqn (1), k_{COOH} and k_{COO^-} are the rate constants for the reactions of the neutral and anionic forms of esters **1a–d**, respectively, and K_a represents the acid dissociation constants of **1a–d**, k_H denotes the second order rate constant for the hydronium ion catalyzed reaction. Since the hydroxide reaction is unimportant between pH 1–6, it can be neglected. The solid lines in Fig. 2 were calculated

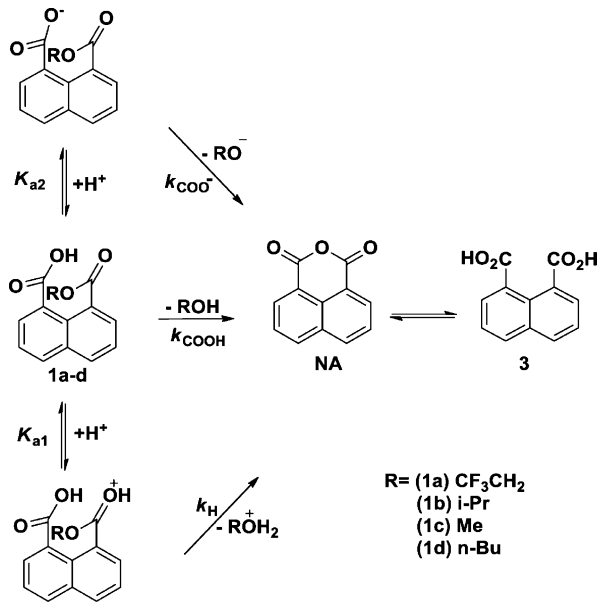

Scheme 3 Possible reaction paths and species involved in the decomposition of alkyl monoesters of 1,8-naphthalic acid.

using eqn (1) and the apparent kinetic pK_a values obtained for all four compounds are consistent with the value of 3.82 ± 0.03 measured by the spectroscopic titration of compound **1c** (at 25 °C, see supplementary information, Fig. S2†) and the reported pK_a of 3.5 for the parent 1,8-naphthalic acid (Table 1).[5a]

Table 1 summarizes the rate and dissociation constants used for fitting the pH–rate profiles. The rate constants k_{COOH} show the individual contributions to the anchimeric assistance of the carboxylic acid in the transacylation reaction. The carboxylate anion is efficient when the less basic 2′,2′,2′-trifluoroethoxide is the leaving group of the naphthalic acid monoester (**1a**)[5b] and does not contribute significantly with compounds **1b–d**. Conversely, the reactivity of the carboxylic acid form is fully functional even when more basic and, therefore, less efficient leaving groups are involved (**1b–d**). The rate constants for the hydronium ion catalyzed reaction (k_H) are of the same order of those reported for the reaction of aspirin derivatives[7] and are consistent with a partial contribution of the specific acid catalyzed pathway described in Scheme 3.

Activation parameters for the hydrolysis of esters **1a–d** are shown in Table 2. Enthalpies of activation fall in the range reported for the related hydrolysis of methyl hydrogen dialkylmaleates.[9] However, compounds **1a–d** show negative entropies of activation substantially lower than the corresponding values for dialkylmaleates[9] which is indicative of a reaction involving a bimolecular process.[10]

Significantly, the observed solvent kinetic isotope effect (SKIE) depends markedly on the species present in solution, with a SKIE $k_{H_2O}/k_{D_2O} = 1.01$ reported for compound **1a** in the plateau region above pH 4,[5b] strongly indicative of nucleophilic attack by the carboxylate anion. The same ester **1a**, at pH 0, shows a SKIE $k_{H_2O}/k_{D_2O} = 1.47$, which indicates proton transfer, but the observed SKIE may contain contributions of the acid catalysis and the remaining reactivity of the monoanion. Conversely, the SKIE observed for the alkyl esters **1b–d**, measured in the plateau region of the carboxylic acid form at pH 2.0 (pD 2.50 at 50 °C[11]), shows k_{H_2O}/k_{D_2O} values in the range between 2.50 and 2.88 and the magnitude of the SKIE is fully consistent with the involvement of proton transfer in the rate-determining step.

The rate constants for assistance by the neighboring COOH groups show a small dependence on the pK_a of the leaving group (Fig. 3). The exceptional level of reactivity observed for compounds **1a–d** is specific to enzymatic and intramolecular reactions where the reacting groups are held close together; as they are in 1,8-naphthalene derivatives.[12] Our results are consistent with those reported by Thanassi and Bruice[13] for hydrolyses of monoalkyl esters of phthalic acid, and by Kirby and coworkers[9] for hydrolyses of alkyl hydrogen dialkylmaleates. In fact, hydrolysis of compound **1c** shows a significant general base catalysis in the presence of chloroacetate buffer (Fig. S4†) and this result is consistent with an addition elimination mechanism, similar to that proposed for the hydrolysis of methyl hydrogen diisopropylmaleates.[9]

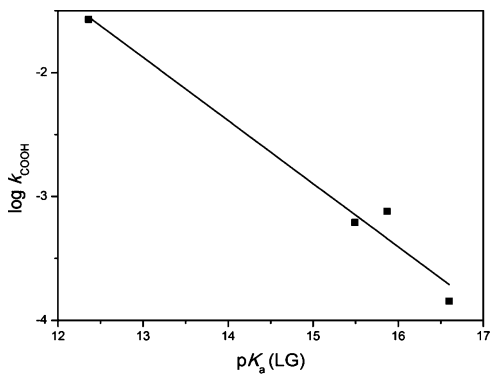

Fig. 3 Linear free-energy relationships between the log of the rate constant and the pK_a of the leaving group for the participation of neighboring COOH (■) groups in the hydrolysis of esters **1a–d** at 50 °C.

The value of $\beta_{LG} = -0.50$ for the reaction involving catalysis by the COOH group indicates that the reaction is sensitive to the basicity of the leaving group. Nucleophilic catalysis in the region where the carboxylate anion is the predominant species becomes important when the nucleophile is more basic than

Table 1 Rate constants for carboxylic and carboxylate catalysis in ester hydrolysis at 50° C

Ester	pK_a	pK_a (LG)	k_{COOH} (10^{-4} s^{-1})	k_{COO^-} (s^{-1})	k_H (10^{-4} $M^{-1}s^{-1}$)
1a[a]	3.83 ± 0.02[a]	12.36[b]	268.7[c]	0.15 ± 0.01[a]	1.15 ± 0.02[a]
1b	4.45 ± 0.33	16.60[d]	1.43 ± 0.25	—	1.83 ± 0.01
1c	4.37 ± 0.17	15.49[d]	6.15 ± 0.12	—	3.62 ± 0.06
1d	4.26 ± 0.16	15.87[d]	7.57 ± 0.70	—	3.27 ± 0.04

[a] From ref. 5b measured at 20 °C. [b] From ref. 8. [c] Rate constant given in the Eyring plot in the Supplementary Information.† [d] From ref. 9.

Table 2 Activation parameters for hydrolysis of naphthalic acid monoesters in the pH ranges for catalysis by carboxylic acid groups at 50 °C

Ester	pH	$\Delta H^{\ddagger}$,[a] kcal mol^{-1}	$\Delta S^{\ddagger}$,[b] cal mol^{-1}K^{-1}	$\Delta G^{\ddagger}$,[c] kcal mol^{-1}	(k_{H_2O}/k_{D_2O})
1a	0	15.2	−18.9	21.3	1.47[d]
1b	2.0	16.0	−26.6	24.6	2.54
1c	2.0	15.9	−24.1	23.7	2.88
1d	2.0	15.4	−25.3	23.6	2.50

[a] Calculated from the Eyring plots shown in Fig. S3.† [b] Calculated from $\Delta S^{\ddagger} = (\Delta H^{\ddagger} - \Delta G^{\ddagger})/T$, where T is the temperature. [c] Estimated from $\Delta G^{\ddagger} = RT \ln[k_B T/(hk_{COOH})]$, where k_B and h are the Boltzmann and Planck constants, respectively. [d] Measured at 20 °C.

the leaving group by at least 3–4 pK_a units.[14] Similarly, in the hydrolysis of aspirin the neighboring carboxylate anion functions as a general base, and nucleophilic attack by the carboxylate anion is only observed for the 3,5-dinitroaspirin derivative, a compound with a much better leaving group.[15] The enforced proximity of the carboxylate anion in 1,8-naphthalic acid derivatives **1a–d** allows the observation of a significant nucleophilic reaction even when the pK_a of the leaving group is as high as 12.36 (2,2,2-trifluoroethanol).[9] The exceptional reactivities of the COOH and COO^- forms in intramolecular reactions depends on the orientation and proximity of the reacting groups, which is close to a maximum in the alkyl monoesters **1** of 1,8-naphthalic acid. A similar behavior was reported for the hydrolysis of **1AC2NA** anion, where, despite the relatively high basicity of the naphthoate leaving group, the carboxylate group acts as a nucleophile rather than a general base (Scheme 4).[10]

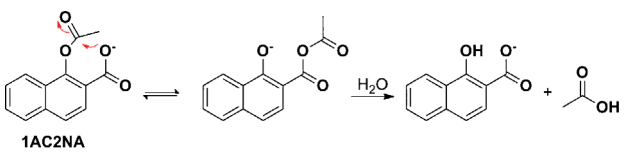

Scheme 4 Nucleophilic attack by the carboxylate group in **1AC2NA**.

In enzymatic systems, decreasing the effective distances between groups reacting in the active site should enhance the reactivity of a carboxylate/carboxylic acid system, which could be ultimately involved in the hydrolysis of a variety of esters and amides. In fact, many of the aspartic proteinases function as digestive enzymes with two aspartic acid residues, one acting as a general acid and the other as a carboxylate anion.[1a]

2.1 Theoretical calculations

The high level of intramolecular reactivity observed in the cyclization reactions of the 1,8-naphthalic acid monoesters must certainly be related to the special structure of the naphthalene derivatives. To improve our understanding of the structures of reactants, transition states and intermediates we performed computational calculations at the B3LYP/6-31+g(d) level on the hydrolysis of the COOH form of the methyl ester **1c**, including one explicit water molecule to help account for the observed isotope effect which suggests that the mechanism of the COOH-catalyzed reaction is likely to involve H_2O as a reagent.

Fig. 4 shows the calculated structures of the main species involved in the decomposition of the methyl ester **1c**. Starting from the ester–water complex (**1c·H$_2$O**) we located **TS1**, leading to the tetrahedral intermediate–water complex (**IT·H$_2$O**), which is subsequently decomposed to methanol, water and naphthalic anhydride (**NA**) through **TS2** according to Scheme 5.

The most significant geometrical parameters of the calculated structures are given in Table 3. The calculated structures shown in Fig. 4 are consistent with those previously reported for the trifluoroethyl ester **1b**[5b] and show the expected rigid, highly strained aromatic system for the reactant. The structure **1c·H$_2$O** (Fig. 4) has the nucleophilic carbonyl oxygen of the COOH group only 2.75 Å from the ester carbonyl carbon, positioned to lie well within the π*-region of the C═O bond, with a near ideal Dunitz "attack angle" of 105.8°. The reactant structure shows significant strain from the eclipsing interaction of the two carboxyl groups, in the shape of significant distortions from planarity. Thus the carbonyl carbons C1 and C5 lie 0.46 Å and 0.51 Å, respectively, above and below the mean plane formed by the ring carbons (C2, C3 and C4 were excluded because of the strong distortion). Not only are the positions of carbons C1 and C5 distorted: so too is the dihedral angle C2–C3–C4–C6 of the naphthalene ring-system. At approximately 7.75° this accounts for the large difference in energy between **1c·H$_2$O** and the anhydride **NA**. The anhydride is planar, with no repulsions between carbonyl groups, thus providing a significant driving force for the strong intramolecular catalysis.

Fig. 5A and 5B show the changes in bond lengths involving **TS1** and **TS2**, respectively. As shown in Fig. 5A, proton transfer plays a fundamental role in the decomposition of the reactant ester and the attack of O1 on C1 is concerted with proton transfer from O1 to water, which then donates H2 to O3. Thus, the water molecule acts as both a general base and a general acid in the intramolecular

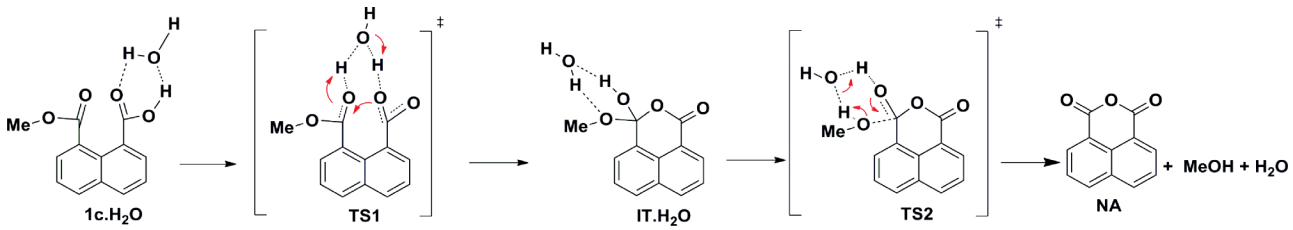

Scheme 5 Hydrolysis of monoester **1c** consistent with the computational results.

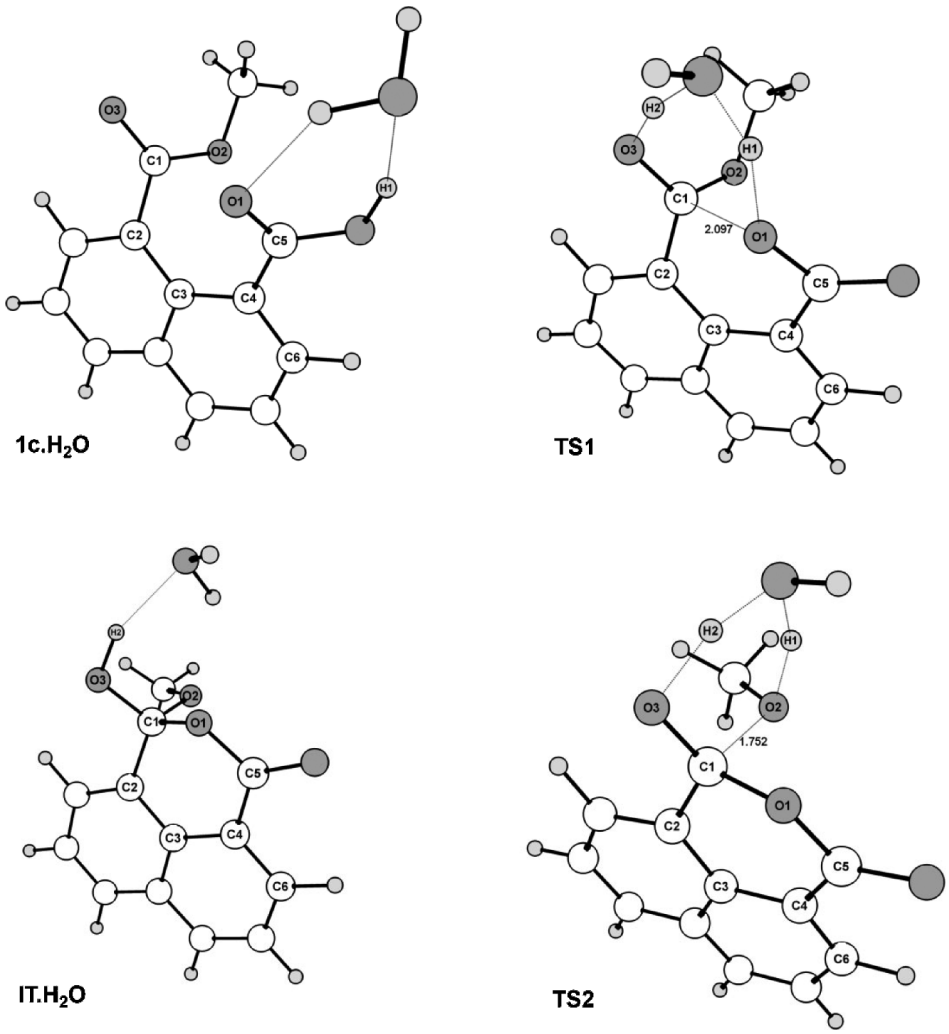

Fig. 4 Structures of **1c·H$_2$O**, **TS1**, **IT·H$_2$O** and **TS2** calculated at the B3LYP/6-31+g(d) level for the hydrolysis of the neutral methyl monoester of 1,8-naphthalic acid. Cartesian coordinates are given in the Supporting Information.†

Table 3 Selected distances (Å) for the optimized structures in the decomposition of **1c·H$_2$O** to **MeOH+H$_2$O+NA** at the B3LYP/6-31+g(d) level. Numbering according to Fig. 4

Structure	O1–C1	C1–O2	C1–O3	O3–H2	O1–H1	O2–H1
1c·H$_2$O	2.75	1.35	1.21		2.32	3.76
IT·H$_2$O	1.44	1.44	1.37	0.99	—	—
TS1	2.10	1.33	1.28	1.21	1.47	3.20
TS2	1.42	1.75	1.28	1.32	2.55	1.31
NA	1.39	—	1.21		—	—
MeOH	—	—	—		—	0.97

attack of O1 on C1, activating in turn the carboxylic acid and the ester carbonyl groups. The formation of **IT·H$_2$O** *via* **TS1** involves an increase in the O1–H1 distance, with O1–C1 and O3–H2 distances falling from 2.10 Å and 1.21 Å in **TS1** to 1.44 Å and 0.99 Å in **IT·H$_2$O**, respectively (see Table 3).

The variations of bond lengths shown in Fig. 5B also indicate the essential role of proton transfers as methoxide departure is assisted by the incipient hydronium ion. In product formation *via* **TS2**, the O2–H1 bond length decreases while those of O3–H2 and C1–O2 increase, giving methanol, naphthalic anhydride and water. Thus the water molecule also plays fundamental roles as both a general base and a general acid in the reaction *via* **TS2**, assisting the formation of the anhydride carbonyl groups and the loss of methanol.

Fig. 6 shows the calculated solution free energy ($G_{solution}$) relative to **1c·H$_2$O** involving the structures in Fig. 4 and Scheme 5. The higher barrier is **TS2** and the calculated and experimental values (27.9 and 23.0 kcal mol^{-1}, respectively) for hydrolysis of **1c** are in good agreement. The product formation is highly exothermic due to release of the steric strain of the *peri*-substitiuents in **1c·H$_2$O**

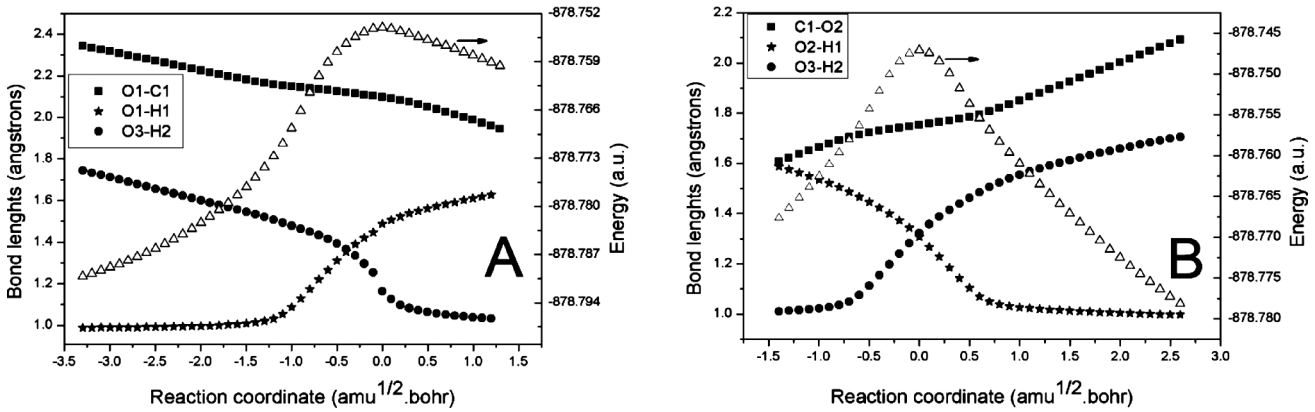

Fig. 5 Variation of bond lengths and energies (△) along the IRC for the hydrolysis of **1c**·H_2O involving (**A**) **TS1** and (**B**) **TS2**.

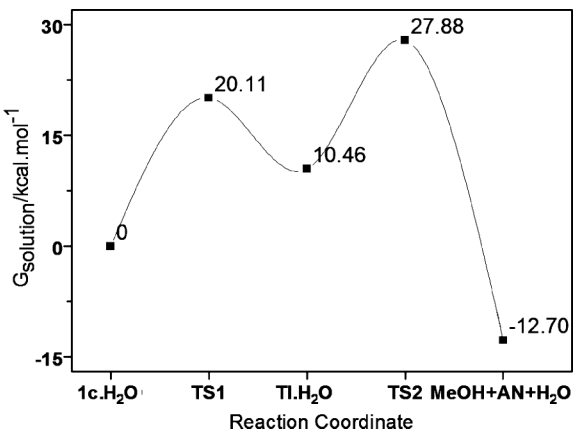

Fig. 6 Gibbs free energy in solution (relative to **1c**·H_2O reactant) for the species involved in the hydrolysis of **1c** calculated with the B3LYP/6-31+g(d) method.

going on to the planar aromatic system in **AN**. The kinetic solvent isotope effect in the hydrolysis of **1c** is consistent with proton transfer in the reaction through **TS2**.

It is interesting to note that, consistent with the lower reactivity of the anionic form of **1c**, due to the high energy inherent to methoxide as leaving group in the gas phase, all attempts to find a minimum energy in the calculation failed, even with inclusion of 2, 3 and even 4 explicit water molecules hydrogen bonded to the departing methoxide ion.

3. Conclusions

The hydrolysis of alkyl 1,8-naphthalic acid monoesters proceeds with efficient intramolecular catalysis by both neighboring COOH and carboxylate groups and the reactivity depends on leaving group pK_a, with a β_{LG} value of –0.50 being observed for the neighboring COOH group. The release of the steric strain of the *peri*-substituents in the highly reactive alkyl 1,8-naphthalic acid monoesters is fundamental to understand the observed special reactivity in this intramolecular reaction. The intramolecular efficiency of the observed reaction is comparable with the fundamental contribution of the carboxylate/carboxylic acid system in aspartic proteinases, where the aspartic acid residues act as a general acid and carboxylate anion, respectively.[1a] The experimental results and the theoretical calculations are consistent with a mechanism involving rate determining breakdown of a tetrahedral addition intermediate. Calculations show that the cleavage of the neutral ester can be catalyzed by water, which plays fundamental roles as both a general base and a general acid in the reaction.

4. Experimental

All chemicals were of reagent grade and were used as received. ESI analyses were performed with interface, CDL and block temperatures set at 250, 250 and 200 °C, respectively. The detector was maintained at 1.50 kV, the flow of N_2 at 1.5 L min^{-1} and the mobile phase was 2 : 8 MeOH/H_2O. The ester concentration in the samples was about 10^{-5} M. Chemical shifts, δ, ppm, are relative to internal TMS.

Attempts to isolate the individual esters failed due to its reactivity, giving the corresponding anhydride. Thus, all compounds were characterized in solution as the triethylammonium salt by mixing 10 mg of **AN** with 5 eq. of the respective alcohol and 2 eq. of triethylamine in MeOD (for compound **1c**) or CD_3CN (for compounds **1b** and **1d**). Typical HPLC analyses, realized prior to the kinetic runs, are given in Fig. S5†.

4.1 Synthesis

4.1.1 Butyl monoester of 1,8-naphthalic acid (1d). To a solution containing 0.198 g (1.0 mmol) of 1,8-naphthalic acid in 20 mL of butanol at 50 °C was added 0.21 mL (1.5 mmol) of triethylamine, and the reaction was maintained under stirring for 6 h. ^{1}H NMR (400 MHz, CD_3CN): δ 0.92 (t, J = 7.0 Hz, 3H), 1.02 (t, J = 7.2 Hz, 9H), 1.37 (m, J = 7.0 Hz, 2H), 1.71 (quint, J = 7.0, 2H), 2.55 (q, J = 7.2, 6H), 4.24 (t, J = 7.0, 2H); 7.50 (dd, J = 8.2, 7.1 Hz, 1H), 7.51 (dd, J = 8.2, 7.1 Hz), 7.78 (dd, J = 7.1, 1.4 Hz, 1H); 7.89 (dd, J = 8.2, 1.4 Hz, 1H); 7.94 (dd, J = 7.1, 1.4 Hz, 1H); 8.01 (dd, J = 8.2, 1.4 Hz, 1H). ESI-MS negative-ion mode: m/z (%): calc for $C_{16}H_{15}O_4^-$: 271.10; found: 271.05 (100).

4.1.2 Methyl monoester of 1,8-naphthalic acid (1c). To a solution containing 0.198 g (1.0 mmol) of 1,8-naphthalic acid in 20 mL of methanol at 25 °C was added 0.21 mL (1.5 mmol) of triethylamine, and the reaction was maintained under stirring for 6 h. ^{1}H NMR (400 MHz, CD_3OD): δ 1.15 (t, J = 7.3 Hz, 9H), 2.88

(q, J = 7.3, 6H), 3.88 (s, 3H), 7.51 (t, J = 7.6 Hz, 2H); 7.83 (dd, J = 7.1, 1.3 Hz, 1H); 7.88 (dd, J = 7.1, 1.3 Hz, 1H); 7.91 (dd, J = 8.2, 1.3 Hz, 1H); 8.03 (dd, J = 8.2, 1.3 Hz, 1H). ESI-MS negative-ion mode: m/z (%): calc for $C_{13}H_9O_4^-$: 229.05; found: 229.05 (100).

4.1.3 *n*-Isopropyl monoester of 1,8-naphthalic acid (1b). To a solution containing 0.198 g (1.0 mmol) of 1,8-naphthalic acid in 20 mL of isopropanol at 50 °C was added 0.21 mL (1.5 mmol) of triethylamine, and the reaction was maintained under stirring for 12 h. ^{1}H NMR (400 MHz, CD_3CN): δ 1.02 (t, J = 7.2 Hz, 9H), 1.18 (d, J = 6.0 Hz, 3H), 1.36 (d, J = 6.3 Hz, 3H), 2.55 (q, J = 7.2 Hz, 6H), 5.14 (quint, J = 6.2, 1H), 7.50 (dd, J = 8.2, 7.1 Hz, 1H), 7.51 (dd, J = 8.2, 7.1 Hz, 1H), 7.78 (dd, J = 7.1, 1.4 Hz, 1H); 7.89 (dd, J = 8.2, 1.4 Hz, 1H); 7.94 (dd, J = 7.1, 1.4 Hz, 1H); 8.01 (dd, J = 8.2, 1.4 Hz, 1H). ESI-MS negative-ion mode: m/z (%): calc for $C_{15}H_{13}O_4^-$: 257.10; found: 257.00 (100).

4.2 Kinetics

Rates of formation of the anhydrides from monoesters of 1,8-naphthalic acid were followed on a spectrophotometer coupled with a thermostated water-jacketed cell holder. All solutions were prepared with CO_2 free distilled, demineralized water which was boiled and cooled under nitrogen. Reactions were initiated by injection of 10 μL of *ca.* 10 mM solutions of substrates into 3 mL of buffer solutions. Absorbance *versus* time data were stored directly on a microcomputer and first-order rate constants (k_{obs}) were calculated from linear plots, at the wavelength maximum of 340 nm, of $\ln(A_\infty - A_t)$ against time for at least 90% reaction by using an iterative least-squares program; correlation coefficients (r) were > 0.999 for all kinetic runs. At conditions where the rate constant for **NA** hydrolysis is similar to its formation, absorbance *vs.* time data were fitted with eqn (2), according to Scheme 6,[5a] with $k_1 \neq k_2$.

$$\mathrm{Abs} = [\mathrm{Ester}]_0 \left\{ 1 + e^{-k_1 t} + \frac{k_1(e^{-k_1 t} - e^{-k_2 t})}{k_2 - k_1} + \frac{k_2 e^{-k_1 t} - k_1 e^{-k_2 t}}{k_1 - k_2} \right\} \quad (2)$$

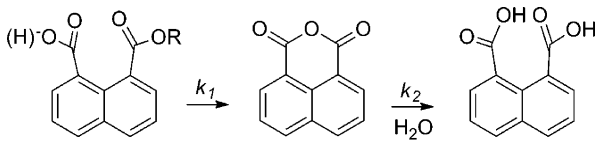

Scheme 6

4.3 Computational methods

Gaussian 03 (Revision D.01)[16] program was used for all calculations. The B3LYP[17] hybrid functional with the 6-31+G(d) basis set was employed and the stationary points were verified by calculating the Hessians matrix, where the minimum energy structures have no imaginary frequency and transition state structures have one imaginary frequency. To obtain a deeper insight into the reaction mechanism, we calculated the intrinsic reaction coordinate (IRC)[18] using the Gonzalez–Schlegel second-order path,[19] starting from the optimized transition-state structure, with a step length of 0.01 a.m.u.$^{1/2}$ (Bohr). The solvent effects on the energetic results obtained in gas phase were included by means of the polarizable continuum model (PCM)[20] on single point calculations, with the molecular cavity computed, including explicit hydrogens, with the UFF radius[21] allowing calculation of the Gibbs solvation free energy ($\Delta G^{solvation}$). Using a simplified model (PCM) to describe solvation effects does not account for specific solvent–solute interactions (*e.g.* hydrogen bonds) that are certainly important in this particular reaction in aqueous solution. Therefore, in all calculations, we included one water molecule to begin to account for the kinetic solvent isotope effect observed experimentally. The total free energy in solution ($G_{solution}$) was calculated by summing the electronic and thermal free energies to $\Delta G^{solvation}$. For conversion from 1 atm standard state to 1 mol L^{-1} standard state, ΔG_{eq} from **1c·H$_2$O** to **MeOH+H$_2$O+NA** shown in Fig. 6 was corrected[22] by adding 3.79 kcal mol^{-1} to the calculated value according to an A → B + C + D reaction. For structures of **1c·H$_2$O** and **TI·H$_2$O** the basis set superposition error (BSSE) was estimated using the Counterpoise method[23] implemented in Gaussian 03. Theoretical calculations for cyclization involving a number of explicit water molecules, although possible, were not of interest for this work.

Acknowledgements

We are grateful to INCT-Catálise, PRONEX, FAPESC, CNPq, and CAPES for support of this work.

Notes and references

1 (*a*) *From enzyme models to model enzymes*, A. J. Kirby and F. Hollfelder, RSC Publishing, Cambridge, 2009; (*b*) F. M. Menger and M. Ladika, *J. Am. Chem. Soc.*, 1988, **110**, 6794–6796; (*c*) A. J. Kirby, *Acc. Chem. Res.*, 1997, **30**, 290–296; (*d*) V. G. Machado and F. Nome, *Chem. Commun.*, 1997, 1917–1918; (*e*) V. G. Machado, C. A. Bunton, C. Zucco and F. Nome, *J. Chem. Soc., Perkin Trans. 2*, 2000, 169–173.

2 (*a*) D. L. Rabenstein, T. S. Shi and S. Spain, *J. Am. Chem. Soc.*, 2000, **122**, 2401–2402; (*b*) C. Cox and T. Lectka, *J. Am. Chem. Soc.*, 1998, **120**, 10660–10668; (*c*) K. Bowden and A. Brownhill, *J. Chem. Soc., Perkin Trans. 2*, 1997, 219–221; (*d*) F. Hollfelder, A. J. Kirby and D. S. Tawfik, *J. Org. Chem.*, 2001, **66**, 5866–5874; (*e*) N. Asaad and A. J. Kirby, *J. Chem. Soc., Perkin Trans. 2*, 2002, 1708–1712.

3 (*a*) *Structure and Mechanism in Protein Science: A Guide to Enzyme Catalysis and Protein Folding, 1st Edition*, A. R. Fersht and W. H. Freeman, New York, 1998; (*b*) A. B. Onofrio, A. C. Joussef and F. Nome, *Synth. Commun.*, 1999, **29**, 3039–3049; (*c*) A. B. Onofrio, J. C. Gesser, A. C. Joussef and F. Nome, *J. Chem. Soc., Perkin Trans. 2*, 2001, 1863–1868; (*d*) Z. J. Wu, F. Q. Ban and R. J. Boyd, *J. Am. Chem. Soc.*, 2003, **125**, 3642–3648.

4 A. J. Kirby, N. Dutta-Roy, D. da Silva, J. M. Goodman, M. F. Lima, C. D. Roussev and F. Nome, *J. Am. Chem. Soc.*, 2005, **127**, 7033–7040.

5 (*a*) T. C. Barros, S. Yunes, G. Menegon, F. Nome, H. Chaimovich, M. J. Politi, L. G. Dias and I. M. Cuccovia, *J. Chem. Soc., Perkin Trans. 2*, 2001, 2342–2350; (*b*) S. F. Yunes, J. C. Gesser, H. Chaimovich and F. Nome, *J. Phys. Org. Chem.*, 1997, **10**, 461–465.

6 (*a*) E. S. Orth, T. A. S. Brandao, B. S. Souza, J. R. Pliego, B. G. Vaz, M. N. Eberlin, A. J. Kirby and F. Nome, *J. Am. Chem. Soc.*, 2010, **132**, 8513–8523; (*b*) M. Silva, R. S. Mello, M. A. Farrukh, J. Venturini, C. A. Bunton, H. M. S. Milagre, M. N. Eberlin, H. D. Fiedler and F. Nome, *J. Org. Chem.*, 2009, **74**, 8254–8260; (*c*) E. S. Orth, P. L. F. da Silva, R. S. Mello, C. A. Bunton, H. M. S. Milagre, M. N. Eberlin, H. D. Fiedler and F. Nome, *J. Org. Chem.*, 2009, **74**, 5011–5016; (*d*) E. S. Orth, T. A. S. Brandao, H. M. S. Milagre, M. N. Eberlin and F. Nome, *J. Am. Chem. Soc.*, 2008, **130**, 2436–2437; (*e*) J. B. Domingos, E. Longhinotti, T. A. S. Brandao, L. S. Santos, M. N. Eberlin, C. A. Bunton and F. Nome, *J. Org. Chem.*, 2004, **69**, 7898–7905; (*f*) J. B. Domingos, E. Longhinotti, T. A. S. Brandao, C. A. Bunton, L. S. Santos, M. N. Eberlin and F. Nome, *J. Org. Chem.*, 2004, **69**, 6024–6033.

7 A. R. Fersht and A. J. Kirby, *J. Am. Chem. Soc.*, 1968, **90**, 5818.
8 P. Ballinger and F. A. Long, *J. Am. Chem. Soc.*, 1959, **81**, 1050–1053.
9 M. F. Aldersley, A. J. Kirby and P. W. Lancaste, *J. Chem. Soc., Perkin Trans. 2*, 1974, 1504–1510.
10 B. S. Souza and F. Nome, *J. Org. Chem.*, 2010, **75**, 7186–7193.
11 T. H. Fife and T. C. Bruice, *J. Phys. Chem.*, 1961, **65**, 1079–1080.
12 A. J. Kirby and J. M. Percy, *Tetrahedron*, 1988, **44**, 6903–6910.
13 J. W. Thanassi and T. C. Bruice, *J. Am. Chem. Soc.*, 1966, **88**, 747–752.
14 V. Gold, Oakenful. Dg and T. Riley, *J. Chem. Soc. B*, 1968, 515–519.
15 A. R. Fersht and A. J. Kirby, *J. Am. Chem. Soc.*, 1968, **90**, 5818–5826.
16 M. J. Frisch, G. W. Trucks, H. B. Schlegel, G. E. Scuseria, M. A. Robb, J. R. Cheeseman, J. A. Montgomery, Jr., T. Vreven, K. N. Kudin, J. C. Burant, J. M. Millam, S. S. Iyengar, J. Tomasi, V. Barone, B. Mennucci, M. Cossi, G. Scalmani, N. Rega, G. A. Petersson, H. Nakatsuji, M. Hada, M. Ehara, K. Toyota, R. Fukuda, J. Hasegawa, M. Ishida, T. Nakajima, Y. Honda, O. Kitao, H. Nakai, M. Klene, X. Li, J. E. Knox, H. P. Hratchian, J. B. Cross, V. Bakken, C. Adamo, J. Jaramillo, R. Gomperts, R. E. Stratmann, O. Yazyev, A. J. Austin, R. Cammi, C. Pomelli, J. Ochterski, P. Y. Ayala, K. Morokuma, G. A. Voth, P. Salvador, J. J. Dannenberg, V. G. Zakrzewski, S. Dapprich, A. D. Daniels, M. C. Strain, O. Farkas, D. K. Malick, A. D. Rabuck, K. Raghavachari, J. B. Foresman, J. V. Ortiz, Q. Cui, A. G. Baboul, S. Clifford, J. Cioslowski, B. B. Stefanov, G. Liu, A. Liashenko, P. Piskorz, I. Komaromi, R. L. Martin, D. J. Fox, T. Keith, M. A. Al-Laham, C. Y. Peng, A. Nanayakkara, M. Challacombe, P. M. W. Gill, B. G. Johnson, W. Chen, M. W. Wong, C. Gonzalez and J. A. Pople, *GAUSSIAN 03 (Revision D.01)*, Gaussian, Inc., Wallingford, CT, 2004.
17 (*a*) A. D. Becke, *J. Chem. Phys.*, 1993, **98**, 5648–5652; (*b*) P. J. Stephens, F. J. Devlin, C. F. Chabalowski and M. J. Frisch, *J. Phys. Chem.*, 1994, **98**, 11623–11627; (*c*) S. H. Vosko, L. Wilk and M. Nusair, *Can. J. Phys.*, 1980, **58**, 1200–1211; (*d*) C. T. Lee, W. T. Yang and R. G. Parr, *Phys. Rev. B*, 1988, **37**, 785–789.
18 K. Fukui, *Acc. Chem. Res.*, 1981, **14**, 363–368.
19 (*a*) C. Gonzalez and H. B. Schlegel, *J. Chem. Phys.*, 1989, **90**, 2154–2161; (*b*) C. Gonzalez and H. B. Schlegel, *J. Phys. Chem.*, 1990, **94**, 5523–5527.
20 M. Cossi, V. Barone, R. Cammi and J. Tomasi, *Chem. Phys. Lett.*, 1996, **255**, 327–335.
21 A. K. Rappe, C. J. Casewit, K. S. Colwell, W. A. Goddard and W. M. Skiff, *J. Am. Chem. Soc.*, 1992, **114**, 10024–10035.
22 (*a*) *Thermochemical Kinetics*, S. Benson, Wiley, New York, 1968; (*b*) A. Rastelli, M. Bagatti and R. Gandolfi, *J. Am. Chem. Soc.*, 1995, **117**, 4965–4975.
23 S. Simon, M. Duran and J. J. Dannenberg, *J. Chem. Phys.*, 1996, **105**, 11024–11031.

